EL SEVIER

Contents lists available at ScienceDirect

Global Ecology and Conservation

journal homepage: http://www.elsevier.com/locate/gecco



The impact of host metapopulation structure on short-term evolutionary rescue in the face of a novel pathogenic threat*



Jing Jiao ^{a, *}, Michael A. Gilchrist ^b, Nina. H. Fefferman ^{a, b}

- ^a National Institute for Mathematical and Biological Synthesis, The University of Tennessee, 1122 Volunteer Blvd., Suite 106, Knoxville, TN, 37996. USA
- b Ecology & Evolutionary Biology, The University of Tennessee, 1416 Circle Drive, Knoxville, TN, 37996, USA

ARTICLE INFO

Article history: Received 13 March 2020 Received in revised form 22 June 2020 Accepted 22 June 2020

Keywords: Spatial structure Migration Patch topology Disease-induced mortality SI model

ABSTRACT

While most evolutionary studies of host-pathogen dynamics consider pathogen evolution alone or host-pathogen coevolution, there is evidence that hosts can evolve more rapidly than their pathogen during initial outbreaks after disease introduction, e.g. evolutionary rescue in the short term. In these cases, spatial, temporal and epidemiological factors could all affect the evolutionary dynamics of the host population. To help inform potential conservation policies in the near-term, we considered the case of one pathogen introduced into a metapopulation of hosts with two genotypes: wild type and robust in which there is a tradeoff in disease-driven mortality and spatial mobility. We employed a classic Susceptible-Infected model and explored how differences in mortality and migration affect the representation of host genotypes and total host population persistence. We find that greater difference in disease-driven mortality between the two host types increases the probability of evolutionary rescue, but there is a point after which disease-driven mortality is so high as to drive the disease prevalence below the reproductive threshold, ending the outbreak and therefore benefitting the wild type. Migration reduces the chance of evolutionary rescue by reducing the competition between the two host genotypes when the difference in disease-driven mortality is sufficiently small, but at larger differences migration acts primarily as a facilitator of disease spread, increasing the probability of evolutionary rescue, though significantly decreasing the total size of the surviving population. This study reveals that both epidemiology and metapopulation ecology can play critical roles in host evolution during the emergence of a novel infection and provide guidance for host conservation and disease control.

Published by Elsevier B.V. This is an open access article under the CC BY-NC-ND license (http://creativecommons.org/licenses/by-nc-nd/4.0/).

1. Introduction

Understanding the factors affecting the evolution of host defense and pathogen virulence is crucial for species conservation or disease control (see Anderson and May 1979; Best et al., 2008; Boots and Bowers, 1999; Boots and Haraguchi, 1999; Gillespie, 1975; Payne, 1988; Restif and Koella, 2004). Due to the relatively shorter generation-time of pathogens than hosts (see Bliven and Maurelli, 2012), previous studies often focused on the evolution of pathogens with constant hosts

 $^{^{\}star}\,$ If this manuscript is accepted, the relevant code will be available on GitHub.

^{*} Corresponding author.

E-mail addresses: jjiao3@utk.edu (J. Jiao), mikeg@utk.edu (M.A. Gilchrist), nina.h.fefferman@gmail.com (Nina.H. Fefferman).

(Bremermann and Pickering, 1983; Gordo et al., 2009; Levin and Pimentel, 1981; Wild et al., 2009), or the coevolution between hosts and pathogens (Beck, 1984; Best et al., 2010; Bowers et al., 1994; Carlsson-Granér and Thrall, 2015; Gilchrist and Sasaki, 2002; Lewis, 1981; May and Anderson, 1983).

However, the coevolution of hosts and pathogen is a long-term arms race (Nesse and Williams, 2012). Although pathogens often evolve faster than hosts due to shorter generation times, it is still possible that during any particular time interval (e.g., short-term conservation time period), hosts can exhibit a change in genotype frequencies while the pathogen remains relatively unchanged. For example, in the systems where a new pathogen/or disease invades a naïve host population (e.g., White Nose Syndrome, Ranavirus; see Echaubard et al., 2014; Maslo and Fefferman, 2015), there are abundant susceptible host individuals for pathogens to infect, thus, it is very likely that the hosts would go through strong selection from the pathogen, while initially providing very little selective pressure on the pathogen (see Débarre et al., 2012; Medzhitov et al., 2012). Those novel, invasive diseases are a factor in the survival of species already under threat of extinction from non-disease challenges (e.g. whether or not evolutionary rescue effects may impact the probability of persistence). This means that understanding the impact of diseases on population size and host evolution are critical factors in understanding and planning conservation efforts.

Host population-scale spatial structure (e.g., metapopulation; see Hanski, 1999) would be expected to complicate host-pathogen dynamics (see Laine, 2005; Tack et al., 2014; Thrall and Burdon, 1999; North and Godfray, 2017), and further affects disease transmission and host conservation (e.g., either facilitate gene flow or spread disease; Carlsson-Granér and Thrall, 2006; Carlsson-Granér and Thrall, 2002; Hossack et al., 2020; Maslo and Fefferman, 2015; Sanchez and Hudgens, 2019; Thompson, 1999; Thrall and Burdon, 1999). In those cases, spatial, temporal and epidemiological factors may all potentially influence the evolutionary dynamics of host-pathogen interactions.

Here we built a classic susceptible-infected model to better understand the systems with evolving hosts but constant pathogen and further explore the relative influences of infectious disease epidemiology and host spatial structure (e.g., host metapopulation) on system evolution and conservation in the short term. For simplicity, we only considered two genotypes in host: wild type and robust type, in which robust type is assumed to be the mutant, having higher tolerance (i.e., lower disease-driven mortality; see Best et al., 2008; Miller et al., 2006) once infected and lower mobility than the wild type. We explicitly considered a population that has been recently perturbed (i.e. population size initially is far less than the habitat carrying capacity), but one that could potentially recover unaided in the absence of the introduction of further threat (in this case, from disease), so as to isolate the explicit impacts of the novel pathogen. The host also exhibits a simple metapopulation structure: multiple patches in same environmental conditions with migration of the wild type among patches.

Through this model, we tracked changes in the relative sizes of the two host genotypes (i.e., the size ratio of wild type vs. robust) and total host population size over conservation-relevant time scales. The control parameters we consider are the "mortality ratio" (i.e. the ratio in the disease-driven mortality of infected individuals between wild type and robust type), which is used to represent the epidemiological effect on host evolution, and the "movement rate", which characterizes the influence of host metapopulation dynamics. In addition, patch topology was also studied here to further explore the effect of host spatial structure on the system. Specifically, we first studied the epidemiological effects in isolation: i.e., how the mortality ratio influences host population ratio and total population size of a single patch. We then considered one host metapopulation structure — a closed-loop stepping-stone structure, and further explored the combined effects of host spatial structure and disease epidemiology on the change in host genotypes and total population size. In particular, we first studied the above combined effect by eliminating the case in which the existence of disease in patches largely depends on spreading through host migration (i.e., we assumed that the disease was introduced simultaneously across all patches). We then added the disease spreading (i.e., disease was introduced into one patch and could then spread to other patches through migration) and reanalyzed the above combined effect on system dynamics. Last, we extended our study to multiple patch topological structures and compared the above results to outcomes on different patch topologies. To consider a window during which active interventions and management might be appropriate to preserve such a host population, here we focused on the shortterm system dynamics after the introduction of disease.

2. Methods

We considered a Susceptible-Infected (SI) model to study host-pathogen systems containing one constant pathogen but two host genotypes: wild type and robust type, where robust is assumed to be a mutant, which has lower initial representation in the population but also lower disease-driven mortality, thus, the robust type would be selected for in the presence of disease and eventually replace the wild type entirely, given enough time. We additionally assumed that there is no recovery from infection, so once an individual is infected, it remained infected until dying (whether or not due to infection). When host metapopulation structure was considered, hosts were assumed to exhibit well-mixed interactions in one patch, thus, mating occur among all individuals without regard for host genotypes (i.e., wild type or robust) or epidemiological stages (i.e., susceptible or infected), and both genotypes were equally capable of transmitting infection to all others. All newborns were assumed to be born susceptible. Offspring of within-genotype matings were assigned the genotype of the parents, while offspring of cross-type matings were split such that half of them were assigned to be wild-type susceptibles and the other half were assigned to be robust-type susceptibles.

We also considered the mortality-migration tradeoff (Mittelbach and McGill, 2019; Mordecai et al., 2016; Tilman, 1990) and made the simplifying assumption that only wild type could migrate among patches (thus, the robust type was sedentary

and remained in its natal patch). Therefore, the migration influences on the host population would only come from the wild type. The migration of individual host was assumed to be symmetrical (i.e., individuals have the same chance to migrate in and out of one patch) and individuals could only migrate to the neighboring patches according to patch topology. Migration rate was uniform for all moving individuals and independent of between-patch distance. The carrying capacity of environment was expressed by the limitation on the maximum birth rate every generation (*K*) and the SI dynamics of the two host genotypes were assumed to be same across patches (i.e., there is no environmental heterogeneity among patches). For numerical analysis, all parameters here were assumed to lead to positive numbers of both host types. The detailed model was as follows:

$$\frac{dS_{ji}}{dt} = B_{ji} - \sum_{h \in [M]} \beta_{hi} I_{jh} S_{ji} - \mu_i S_{ji} + m_{ji}^{S}$$
(1)

$$\frac{dI_{ji}}{dt} = \sum_{h \in [W,R]} \beta_{hi} I_{jh} S_{ji} - (\alpha_i + \mu_i) I_{ji} + m_{ji}^I$$
(2)

where the state variables, S_{ji} and I_{ji} are the numbers of susceptible and infected individuals in host genotype i at patch j (i is either W or R, indicating wild type or robust, respectively). β_{hi} describes the transmission from Infected genotype h to susceptible type i, μ_i and α_i are the natural mortality and disease-driven mortality of genotype i. One generation time is equal to $1/\mu_i$. B_{ij} represents all newborns that have genotype i in patch j:

$$B_{ji} = \sum_{h \in [W,R]} L_{S_{ji}S_{jh}} + \sum_{h \in [W,R]} L_{S_{ji}I_{jh}} + \sum_{i \neq h} L_{S_{jh}I_{ji}} + \sum_{h \in [W,R]} L_{I_{ji}I_{jh}}$$

$$(3)$$

in which L describes the babies from random mating combinations (e.g., $L_{S_{il}S_{jh}}$ is the newborn number from the mating between S_{ii} and S_{ih}), which is limited by the maximum number of newborns in patch j (K_i):

$$L_{S_{ji}S_{ji}} = \frac{S_{ji}^2}{P_j} r_i \left(1 - \frac{P_j}{K_j} \right) \tag{4}$$

$$L_{S_{ji}S_{jh}} = \frac{S_{ji}S_{jh}}{P_j} \left(\frac{r_i + r_h}{2}\right) \left(1 - \frac{P_j}{K_j}\right) \text{ where } i \neq h$$
 (5)

$$L_{S_{ji}l_{ji}} = \frac{2S_{ji}l_{ji}}{P_j} \left(\frac{r_i + r_{id}}{2}\right) \left(1 - \frac{P_j}{K_j}\right)$$
 (6)

$$L_{S_{ji}l_{jh}} = \frac{S_{ji}l_{jh}}{P_j} \left(\frac{r_i + r_{hd}}{2}\right) \left(1 - \frac{P_j}{K_j}\right) \quad \text{where } i \neq h$$
 (7)

$$L_{l_{ji}l_{ji}} = \frac{l_{ji}^2}{P_j} r_{id} \left(1 - \frac{P_j}{K_j} \right) \tag{8}$$

$$L_{l_{ji}l_{jh}} = \frac{l_{ji}l_{jh}}{P_j} \left(\frac{r_{id} + r_{hd}}{2}\right) \left(1 - \frac{P_j}{K_j}\right) \quad \text{where } i \neq h$$

$$\tag{9}$$

Here, r_i and r_{id} are the growth rate of susceptible and infected hosts in genotype i, respectively. P_j is the total size of host population (the sum of all susceptible and infected hosts) in patch j:

$$P_{j}(t) = \sum_{i \in [W,R]} S_{ji}(t) + \sum_{i \in [W,R]} I_{ji}(t)$$
(10)

The net immigrations of wild type in either susceptible or infected to patch j are introduced by m_{jW}^S and m_{jW}^I respectively:

$$m_{jW}^{S} = \sum_{k \in [1,N]/\{j\}} \left[mig(k,j)S_{kW} - mig(j,k)S_{jW} \right]$$
(11)

in which mig(k,j) describes the migration from patch k to j ($j \neq k$), depending on the patch topology (i.e. if there is no connection between k and j based on the topological structure, mig(k,j) = 0; if there is a connection, mig(k,j) was equal to the migration rate). m_{jW}^I can be obtained by replacing S by I in m_{jW}^S . Because migration is assumed to be symmetrical, mig(j,k) = mig(k,j).

To study both the separate and combined effects of disease epidemiology and host spatial structure on host dynamics, here we examined how the mortality ratio of wild type vs. robust and the rate of wild type migration affect the number of wild type vs. robust hosts and total population size (the sum of *S* and *I* in both host types) in one isolated patch (which represents the effect only from disease epidemiology) and multiple patches (which indicates the combined effects of both selection and host metapopulation structure) with two disease introduction scenarios: disease is introduced to all patches simultaneously (which allows us to mainly focus on the ecological influences of migration on the system dynamics), or disease is introduced to one focal patch, which was randomly selected from the out layer of each topology, and spreads to others via migration, which would allow us to study the influences of disease spreading through migration on the system. In addition, to better track the size shift between the two host genotypes in the presence of disease across patches, here we chose the parameter values to allow the whole host population to be near the carrying capacity at conservation time scale. We also analyzed and compared the above results across different patch topologies to verify the reliability of our study.

3. Results

3.1. Host dynamics in isolated patch

When patches were isolated, and the mortality ratio was equal to 1 (i.e., no mortality difference between wild and robust type; the solid line in Fig. 1), there was no selection on host genotypes (i.e. see the solid line in Fig. 1a). The whole host population and both host genotypes quickly grew due to demography but started to drop after around 4 generations (see the trend of the solid line in Fig. 1b and in Fig. S1 in Appendix 1) due to the increase in disease prevalence (see the trend of the solid line in Fig. 1c).

When the disease-driven mortality increased in the wild type (e.g., when the mortality ratio increased from 1 to 1.5), the selection on hosts became stronger, especially when the disease prevalence grew to certain size (i.e., after 3 generations). This selection increased the proportion of the disease-resistant, robust host type, leading to a decrease in the size ratio of wild type vs. robust (see the decrease from the solid line to the dashed line in Fig. 1a). The total host population also increased due to evolutionary rescue (see the qualitatively similar patterns between total host population and robust; compare the solid and dashed lines in Fig. 1b and Fig. S1b).

When the disease-driven mortality in wild type became large enough (e.g., when the mortality ratio changed from 1.5 to 2), disease prevalence would largely shrink (compare the dashed and dotted lines in Fig. 1c); thus, the selection on robust became weak, leading to an increase in the size ratio (see the increase pattern from the dashed line to the dotted line in Fig. 1a).

In summary, selection depended on two aspects: the mortality difference between the two host genotypes, and the prevalence of disease. The mortality ratio had threshold effects on host selection: relatively small increases in the mortality ratio would enlarge the mortality difference between wild and robust type, which strengthened the selection on the robust type (i.e. increasing the probability of evolutionary rescue) due to its lower disease-driven mortality than wild type. However, a large increase in the mortality ratio would largely deplete the disease prevalence and weaken the resulting selection on hosts. Therefore, we observed the unimodal pattern on host composition with the increase of the mortality ratio (first decrease but then increase in the size ratio of wild type vs. robust when the mortality ratio increased from 1 to 1.5, from 1.5 to 2 in Fig. 1a).

3.2. Host composition in meta-population

When considering metapopulation dynamics (i.e. more than 1 patch; here we explored metapopulations with 5 patches, which is the minimum number to capture non-trivial topologies; see Greenbaum and Fefferman, 2017), the model included the migration equation (Eq. (11)). Here we first considered a closed loop stepping-stone patch structure (see the stepping stone structure in population genetics studies; see Kimura and Weiss, 1964; Shiga, 1988), but with the two ends wrapped around to meet) and simulated the combined effects of the mortality ratio and migration on the size ratio of the two host genotypes and the corresponding total host population size. We focus, for purposes of conservation efforts on a short time frame (15 generations post disease introduction around 60 years). We then explored whether and how other patch topologies (see Fig. S8 in Appendix 4) influence the above results. We began by exploring the case in which the disease was introduced to all patches simultaneously, in which migration mainly served to increase the gene flow of the wild type, and then presented the alternative case in which disease was introduced to one focal patch only and spreads to others from there through migration.

3.2.1. Closed-loop stepping-stone topology

3.2.1.1. Simultaneous disease introduction in all patches. In this case, disease already existed throughout the entire system, hence, migration mainly influenced the gene flow. Through a competition-colonization tradeoff, migration of the wild type benefited the wild type but decreased the robust type due to the limitation of the carrying capacity (see Fig. S2 and S3 in

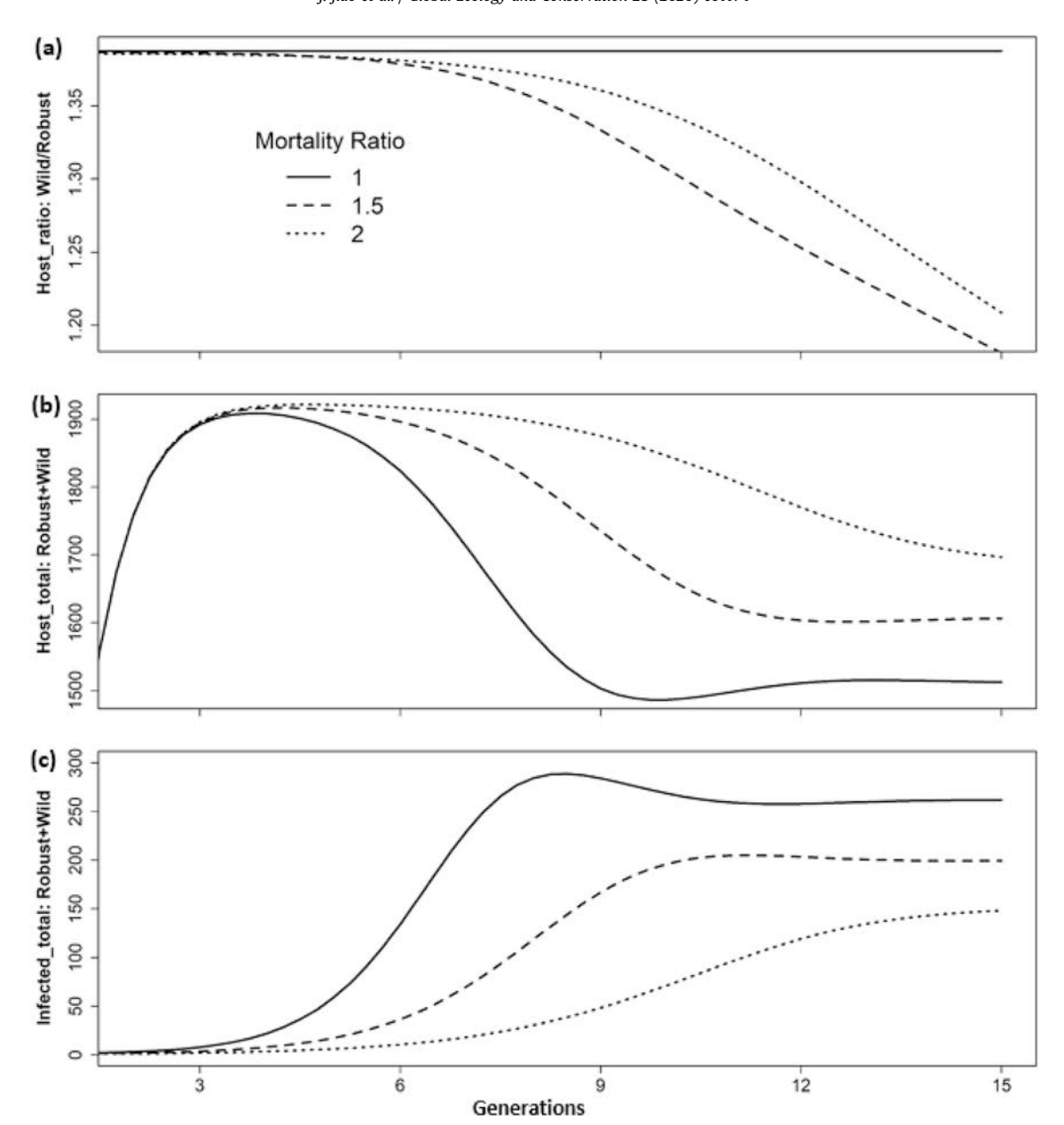


Fig. 1. The dynamics of a) size ratio of two host genotypes (wild type vs. robust), b) total host population (Robust + wild) and c) total infected host size in one isolated patch under three levels of the mortality ratio ($\alpha_W | \alpha_R$): 1 (indicated by the solid line), 1.5 (the dashed line), 2 (the dotted line). The initial numbers of Susceptible are 180 for robust and 260 for wild type. The initial numbers of Infected are 2 for both host genotypes. Both x- and y-axis in a) and b) are truncated to show the main trend of the dynamics. All other parameters are: $r_R = r_W = 0.7$, $r_{Rd} = r_{Wd} = 0.07$, $\alpha_R = 0.25$, $\beta_{RR} = \beta_{RW} = \beta_{WR} = \beta_{WW} = 0.0004$, $\mu_R = \mu_W = 0.25$, and $\mu_R = 0.0000$.

Appendix 2); thus, larger migration of the wild type would increase the size ratio of wild type vs. robust hosts (see the color trend of x-axis of Fig. 2).

Similar to the one-patch model, the mortality ratio had threshold effects on host composition: the increase from 1 to the threshold value (see the red dashed line in Fig. 2) enlarged the mortality difference of the two host genotypes and strengthen the selection favoring the robust type, which decreased the size ratio of wild vs. robust type, thereby exhibiting evolutionary rescue effects. Conversely, the increase from the threshold value to 2 decreased disease prevalence and weaken the selection on the robust type, which increased the size ratio (see the color trend along y-axis in Fig. 2).

The size of the total host population was largely determined by the mortality ratio: with the increase of the mortality ratio, the overall mortality of hosts increased, hence, disease abundance decreased due to the lack of hosts (see the trend along y-axis in Fig. S4), which then boosted the total host population (see the trend along y-axis in Fig. 3). Migration of the wild type

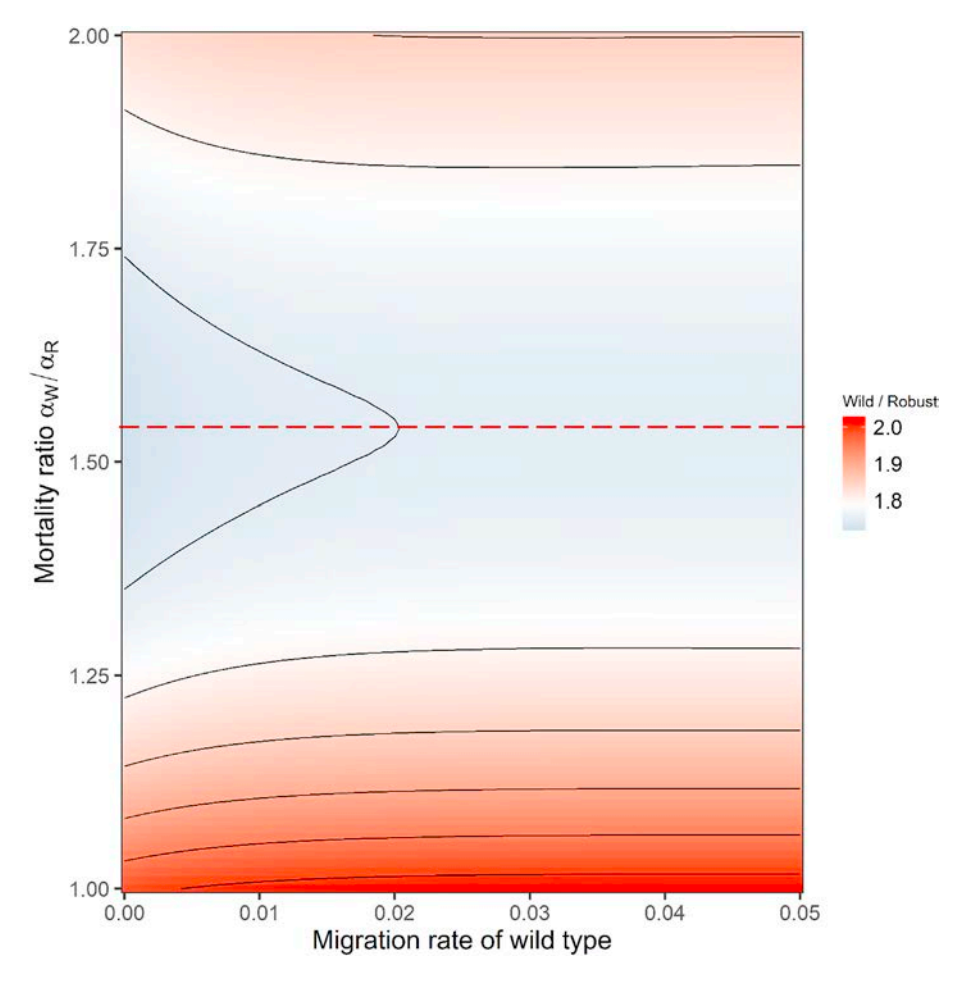


Fig. 2. The change in size ratio of wild type vs. robust hosts (average wild-type number in each patch divided by the average robust number in each patch) under the influences of the migration of the wild type and the mortality ratio (α_W/α_R) after 15 generations (i.e., 60 years) when disease is introduced simultaneously into all patches. The color trend from blue to red shows the increase in the ratio. The initial number of robust susceptible in each patch is one random draw between 100 and 220, while the initial wild-type susceptible is a random draw between 250 and 320. Initial numbers of infected hosts in both types in each patch are 2. All the other parameters are: $r_R = r_W = 0.7$, $r_{Rd} = r_{Wd} = 0.07$, $\alpha_R = 0.25$, $\beta_{RR} = \beta_{RW} = \beta_{WW} = 0.0004$, $\mu_R = \mu_W = 0.25$, and $\kappa = 3000$. The red dashed line indicates the threshold value of the mortality ratio, which shows the trend change. (For interpretation of the references to color in this figure legend, the reader is referred to the Web version of this article.)

changed host composition but did not significantly influence the total population (see the constant color trend along x-axis in Fig. 3).

In summary, when selection from disease was strong (e.g., mortality ratio < the threshold, which was 1.5 in our simulation), the mortality ratio and migration in the wild type had antagonistic effects on shaping host composition: the size ratio of wild vs. robust hosts decreased with the mortality ratio but increased with the migration of the wild type (see the trends under the threshold, i.e., the red dashed line in Fig. 2). However, when selection was weak due to a large mortality ratio (>the threshold), mortality ratio and migration in wild type had synergistic effects on host composition: both would increase the size ratio of wild type vs. robust (see the trends above the threshold mortality ratio in Fig. 2) although the increase of the mortality ratio would increase the absolute sizes of both host genotypes (see the color trend along y-axis of Fig. S2 and S3 in Appendix 2). Given the persistence of total host population, the increase in migration would potentially lead to evolutionary rescue (see Maslo and Fefferman, 2015).

3.2.1.2. Single patch disease introduction in a closed-loop stepping-stone topology. When disease started from one focal patch, even low rates of migration of the wild type would largely decrease the sizes of the host populations with both genotypes (see the sharp drop when migration rates are low along x-axis in Fig. S5 and S6 in Appendix 3) by acting as the mechanism of introduction for the disease to the entire metapopulation structure (see the sudden increase in disease when migration was >0 in Fig. S7 in Appendix 3). As the disease spread, the robust type was selected for due to its lower disease-driven mortality, hence, in general, the increase of migration would lead to a decrease in the size ratio of wild type vs. robust (see the general color trend along x-axis in Fig. 4). However, the migration of wild type could also benefit wild type by reducing its

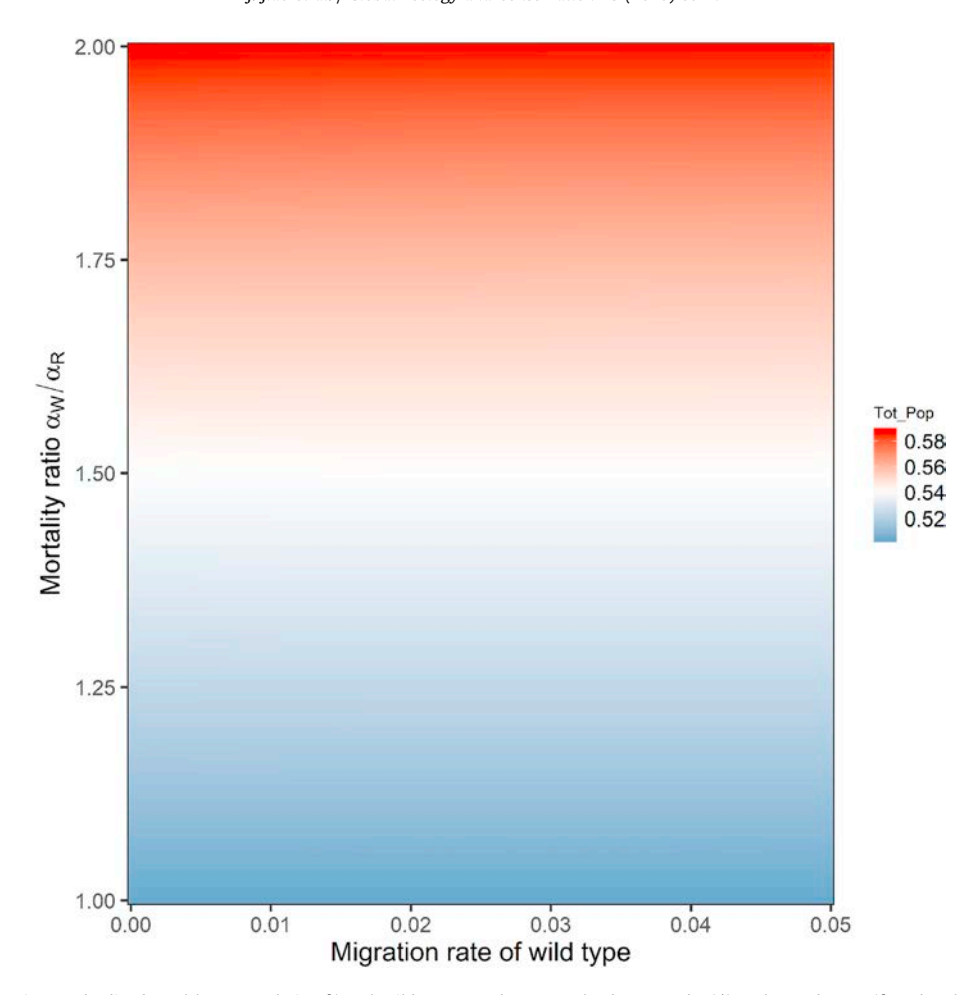


Fig. 3. The change in standardized total host population [(total wild-type number + total robust number)/(patch number * K)] under the influences of the migration of the wild type and the mortality ratio (α_W/α_R) after 15 generations when disease is introduced simultaneously into all patches. The color trend from blue to red shows the increase of host population size. The initial number of robust susceptible in each patch is one random draw between 100 and 220, while the initial number of wild-type susceptible is a random draw between 250 and 320. Initial numbers of infected in both types in each patch are 2. All the other parameters are: $r_R = r_W = 0.7$, $r_{Rd} = r_{Wd} = 0.07$, $\alpha_R = 0.25$, $\beta_{RR} = \beta_{RW} = \beta_{WW} = \beta_{WW} = 0.0004$, $\mu_R = \mu_W = 0.25$, and $\kappa = 0.25$, and $\kappa = 0.25$, $\kappa = 0.25$

competition with the robust type. When disease selection was low, and the abundance of the wild type was relatively high (e.g., when the mortality ratio was near 1), the benefit to the wild type outweighed the selection for the robust type, leading to an increase in the size ratio with migration (see the contour trend near the left bottom of Fig. 4).

The mortality ratio kept a similar unimodal pattern on the size ratio of wild type vs. robust as the one-patch simulation (see the color changed from red to blue, to red again along y-axis in Fig. 4) due to its threshold effects on host composition.

Total population size was largely influenced by disease prevalence. The smaller the infected number was, the larger the host population would be (see the opposite trends between Fig. 5 and Fig. S7 in Appendix 3). Therefore, host population size was high when the mortality ratio was large (which was likely deplete disease) and migration was small (which did not effectively spread the disease) (Fig. 5). Compared to the gradual influence of mortality on disease, migration had an abrupt effect on disease spreading. A small increase in migration would quickly spread the disease from one patch to the entire metapopulation structure (see the sharp color change at a small migration in Fig. 5). Afterward, when the mortality ratio was small (near 1), the increase in migration could largely reduce the competition between the two host types, leading to an increase in total population size (see the contour trend near the bottom of Fig. 5).

3.2.2. Diverse patch topologies

As with the host dynamics in one isolated patch, the average sizes of both host genotypes per patch first increased when disease was still low but decreased once disease prevalence increased. If disease was prevalent, the robust type again

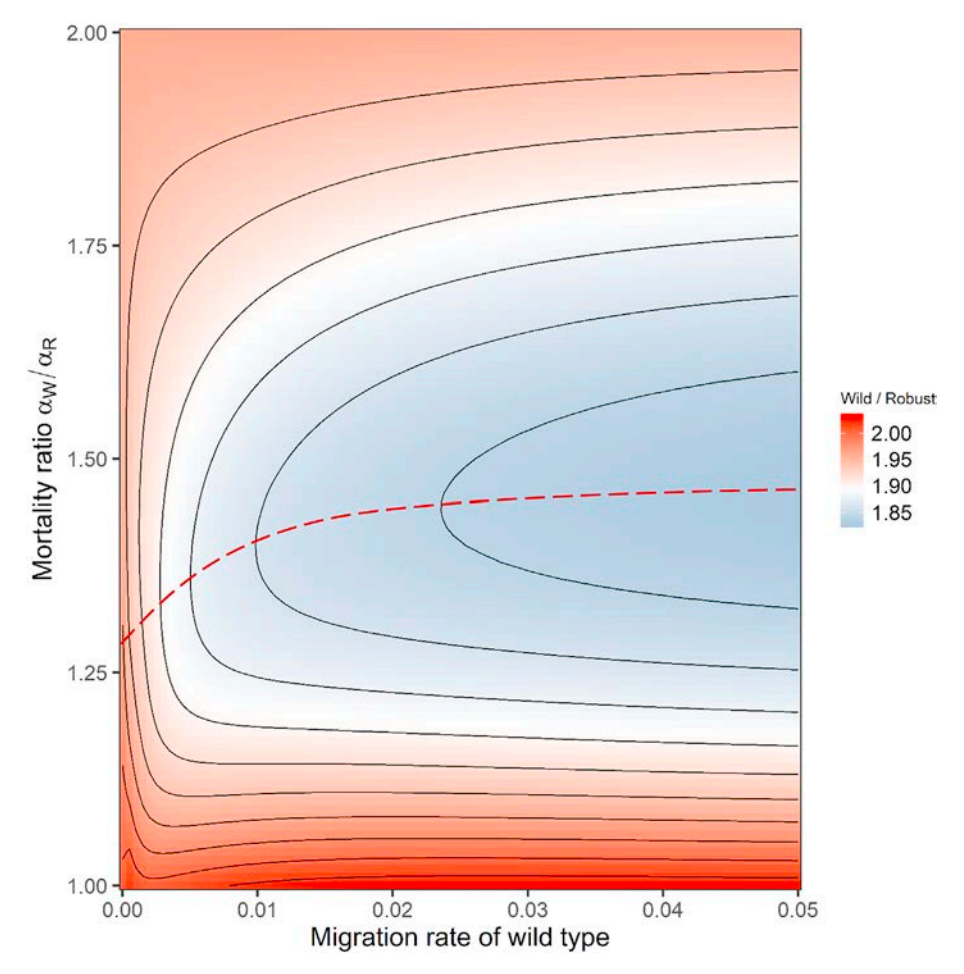


Fig. 4. The change in the size ratio (average wild type vs. robust in each patch) under the influences of the migration of the wild type and the mortality ratio after 15 generations when disease is introduced from one patch. The color trend from blue to red shows the increase of the ratio. The initial number of robust susceptible in each patch is one random draw between 100 and 220, while the initial number of wild-type susceptible is a random draw between 250 and 320. In the patch where disease is introduced, the initial numbers of infected are 2 for both host genotypes. All the other parameters are: $r_R = r_W = 0.7$, $r_{Rd} = r_{Wd} = 0.07$, $\alpha_R = 0.25$, $\beta_{RR} = \beta_{RW} = \beta_{WR} = \beta_{WW} = 0.0004$, $\mu_R = \mu_W = 0.25$, and K = 3000. The red dashed line indicates the threshold value of the mortality ratio, which shows the trend change. (For interpretation of the references to color in this figure legend, the reader is referred to the Web version of this article.)

increased due to selective pressure from the disease, leading to a decrease in the size ratio of wild vs. robust (Fig. S9 and S10 in Appendix 4). The above general pattern was seen across all patch topologies and migration levels.

3.2.2.1. Simultaneous disease introduction in all patches. Similar to the closed-loop stepping-stone topology, all other patch topologies showed that migration would benefit the wild type (see the colored lines above the solid black line in the absence of migration in Fig. S9a) by reducing the competition between the two host genotypes, but would decrease the size of the robust type (see the colored lines below the solid black line in Fig. S9b) due to limitation from the carrying capacity. This led to an increase in the size ratio of wild type vs. robust (see the colored lines above the solid black line in Fig. S9c). The above pattern was qualitatively similar across patch topologies, but the more connected topologies showed stronger patterns (i.e., larger size ratio) than the less connected ones (see the increase in the size ratio when edge number increased with migration < 0.025 in Fig. 6a; compare the blue dotted and red dashed lines in Fig. S9c).

When migration increased, the connections among patches facilitated the synchrony of host-pathogen dynamics across all patches (see the decrease of the size ratio when migration was >0.025 in Fig. 6a), which gradually weakened the effects of migration on host metapopulation dynamics. The extreme case in which migration was extremely large, would mean that all patches were well connected and synchronized as one "larger" patch, leading to the disappearance of between-patch migration; thus, the size ratio would gradually decrease and get closer to that in the absence of migration (see the unimodal pattern across edge numbers along migration in Fig. 6a). More connected patch topologies accelerated the above effects of migration (compare the hump shapes across colors in Fig. 6a).

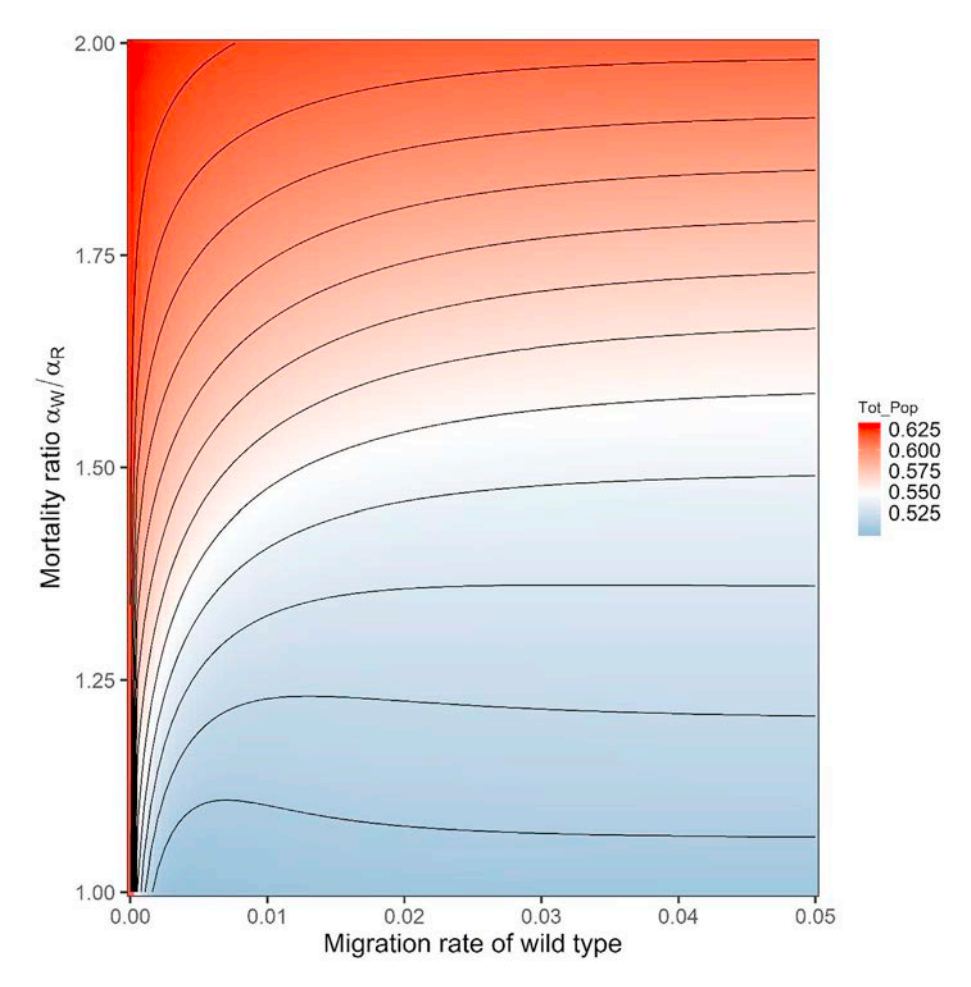


Fig. 5. The change in standardized total host population [(total wild-type number + total robust number)/(patch number * K)] under the influences of the migration of the wild type and the mortality ratio after 15 generations when disease is introduced from one patch. The color trend from blue to red shows the increase of the host population size. The initial number of robust susceptible in each patch is one random draw between 100 and 220, while the initial number of wild-type susceptible is a random draw between 250 and 320. In the patch where disease is introduced, the initial numbers of infected are 2 for both host genotypes. All the other parameters are: $r_R = r_W = 0.7$, $r_{Rd} = r_{Wd} = 0.07$, $r_{Rg} = r_{RW} = r_{$

Similar to the closed-loop topology, host total population sizes in other topological structures were also not sensitive to the change of migration (see the almost overlapped lines in Fig. S9d in Appendix 4).

3.2.2.2. Single patch disease introduction in different patch topologies. When disease started from one patch and spread to other patches, migration of the wild type through patch connections facilitated disease spreading (compare the solid black line and other lines in Fig. S10e Appendix 4). Particularly, the spreading was strengthened by either larger migration or higher patch-connection in the presence of between-patch migration (see the blue dotted and red dashed lines in.)Fig. S10e The disease spreading would introduce extra mortality in hosts, which decreased numbers of hosts with both genotypes and thus the total host population (compare the solid black line with other lines in Fig. S10a, b and din Appendix 3). Due to the increase of selection on hosts, the decrease in the robust type, which was selected for, was lower than the wild type, leading to a decrease in the size ratio of wild type vs. robust with either larger migration or higher patch connection (compare lines in Fig. 6b and Fig. S10c).

The total host population was largely influenced by the disease dynamics: the larger disease led to lower host population (compare the trends in Fig. S10d and S10e). Because disease prevalence increased with larger migration and higher patch connection, total host population decreased when migration in wild type was larger or patch connection was higher (see the lower values of the blue dotted and red dashed line in Fig. S10d).

As would be expected, no matter where disease was introduced (in either all patches or one patch) in the host metapopulation, in the presence of migration, the topologies with more connections (i.e., larger edge numbers) but lower

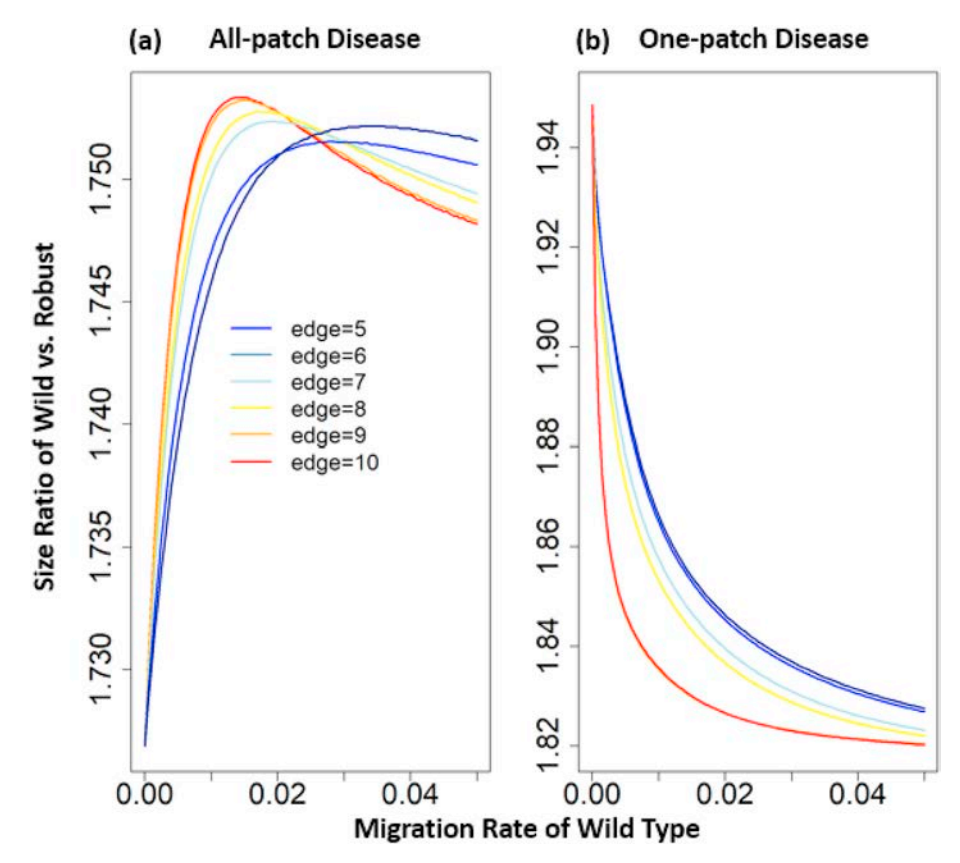


Fig. 6. The influences of topological structures of the host metapopulation (Fig. S9, grouped by edge number) on the size ratio of wild type vs. robust (average wild-type number in each patch divided by the average robust number in each patch) at 1.5 mortality ratio (α_W/α_R) when disease starts from all patches (a) or from one single patch, which is randomly picked from the out layer of each topology (b). From blue to red, the edge number increases. All the other parameters are: $r_R = r_W = 0.7$, $r_{Rd} = r_{Wd} = 0.07$, $r_{Rd} = r_{Wd} = 0.25$, $r_{RR} = r_{RW} =$

migration rates would be equivalent to the topologies that were less connected (with lower edge numbers) but in higher migration rates. Therefore, patch topological connection could facilitate the migration of hosts among patches.

4. Discussion

Once a novel pathogen invades a naïve host population, hosts would likely undergo selection from pathogen (see host evolution in Baalen, 1998; Boots and Bowers, 1999; Boots and Haraguchi, 1999; Didelot et al., 2016; Miller et al., 2005). With the existing host spatial structure, both ecological and epidemiological factors (Conner and Miller, 2004; Earn et al., 1998) would be expected to influence host evolution. Here, with the initially-existing host genotypes, we explored how hosts responded to pathogen selection and provided a mechanistic understanding about the host-pathogen dynamics in systems with evolving hosts and constant pathogens (e.g., White Nose Syndrome and Ranavirus; Echaubard et al., 2014; Maslo and Fefferman, 2015). This study system can be compared to the concept of apparent competition (Holt, 1977). In this case, the two host genotypes act as indirect competitors, with a common "predator" of the novel pathogen.

In general, the increase of the mortality difference between wild type and robust hosts (indicated by the mortality ratio between wild type vs. robust with the fixed mortality in the robust type) would strengthen the disease selection for robust hosts, leading to the decrease in the size ratio of the wild type vs. robust (compare the solid and dashed lines in Fig. 1a; see also the decrease trend of the size ratio along y-axis under the threshold mortality ratio, i.e., the red dashed line in Figs. 2 and 4). The total host population could increase with the increase in the proportion of the robust genotype (Fig. 1a) when the mortality ratio was not large enough to deplete the disease (<the threshold value), i.e., evolutionary rescue occurred (see the similar trend between Fig. 1b and; Fig. S1b see also Carlsson-Granér and Thrall, 2015; Gonzalez et al., 2013; Maslo and Fefferman, 2015). However, when the wild type suffered such great mortality as to largely decrease the disease prevalence in the entire system, the mortality ratio would weaken the selection from disease, leading to an increase in the size ratio (compare the dashed and dotted lines in Fig. 1a and the increase trend of the size ratio when the mortality ratio was > the

threshold value in Figs. 2 and 4). The large decrease in disease prevalence could benefit the total population prevalence (compare Fig. 1b with 1c, Fig. 3 with Fig. S4 and Fig. 5 with). Fig. S7.

When disease started from all patches and the migration of wild type was not large enough to fully synchronize the metapopulation, migration would facilitate the gene flow of the wild type. Given a certain carrying capacity, the patch(es) with larger populations of the robust type would have less space for wild type individuals (i.e., higher competition between the robust and wild types), leading to a higher density of the wild type therein (here we assume equal patch size as 1, which is quantitatively equivalent to Eqs. (1)—(11)). The random movement of wild-type hosts among patches would therefore lead to the net movement of wild type from the patch(es) with high between-type competition (and high wild-type density) to the patches where two host types have lower competition (or lower wild-type density). Therefore, this migration benefits the wild type and increases the size ratio of the wild type vs. robust (Figs. 2 and 6a). The above process can also be understood as a decrease in the encounter rate between the two host types through wild-type migration (see Jiao et al., 2016; Jiao et al., 2018), which also decreases the between-type competition. Here the total host population at 15 generations is limited by the proportion of the total carrying capacity available to each genotype given the mortality ratio (see the trend along y-axis in Fig. 3). This allows us to clearly observe the shift in relative population size between robust and wild type given a particular disease prevalence. Wild-type migration among patches does not influence each patches' carrying capacity, so the total population size does not depend on the migration (see the trend along x-axis in Fig. 3).

When disease started from one patch, a small migration rate could largely facilitate the disease spread across the entire system and increased the total disease prevalence across all patch topologies (Fig. S7 in Appendix 3 and S10e in Appendix 4). However, when the mortality ratio was small (near 1), a further increase in migration would again facilitate the gene flow, reduced the inter-type competition, and boosted the total host population (see the trend near the bottom of Fig. 5). In that case, if the conservation goal is to increase the total host population and disease already spread among patches, building corridors to increase patch connectivity (equivalent to increasing the migration rate; see the exchangeable roles of migration and patch connectivity in Fig. 6a) could benefit host conservation (see Hess, 1996). When the mortality ratio was large, there was reduced prevalence of the disease and migration acted to increase disease persistence by facilitating spread across patches. This resulted in a decrease in the size ratio of wild type vs. robust, i.e. evolutionary rescue occurred (due to the selection on robust type; see Fig. 4). Under this scenario, to protect the host and reduce disease persistence, it may be that conservation strategies should focus on reducing patch connectivity (e.g., block the passway among patches) to decrease migration rate. If disease already spread across all patches and blocking host migration could not sufficiently reduce disease persistence, other strategies considering evolutionary rescue may be applied (see Maslo and Fefferman, 2015).

Due to the advantage of sustained lower mortality, it is very likely that in the presence of sustained, endemic disease transmission would lead to evolutionary rescue, i.e. the robust type would dominate the system as a superior competitor given enough generations, even though the wild type initially had higher number. This is consistent with the classic theory of competition exclusion (Gause, 1970; Levin, 1970). However, this will depend on the relative strengths of migration (or patch connectivity) and differences in disease-driven mortality between the two host genotypes.

To better apply to real systems, some assumptions in our study can be relaxed and studied in future work. For example, we assumed that only the wild type can migrate among patches. Future work could consider mobile mutants and explore the influences of different movement patterns on host evolution (e.g., non-random movement; see Armsworth and Roughgarden, 2005; Jiao et al., 2018). This study also assumed that the host could not recover from infection, which led to long-term disease prevalence (unless the mortality is large enough to decrease the number of infected individuals below the threshold for the effective reproductive value for the disease). Naturally, it will also be important to consider the evolutionary outcomes for diseases from which hosts can recover, either with or without long-lasting immunity against future infection. Also, here we assumed that all patches have similar environmental conditions (i.e., same maximum birth rate and two host genotypes which have slightly different initial sizes but respond consistently across patches). However, in the real world, habitat heterogeneity commonly exists across systems (e.g., Cramer and Willig, 2005; Danielson, 1991; Jiao et al., 2018; Seitz et al., 2017), which may drive very different host-pathogen dynamics in local patches and further influence the pattern in entire system. Future work could include different types of habitat heterogeneity and the potential corresponding movement behaviors. In addition, here we only considered the mortality difference between the host genotypes. Of course, beyond tolerance to the pathogen (Best et al., 2008; Miller et al., 2006), other genetically driven protections for the robust type should be considered, such as increased resistance (i.e., lower transmission and/or increased recovery; see Råberg et al., 2009; Restif and Koella, 2004; Roy and Kirchner, 2000), or longer/more effective immunity (see Débarre et al., 2012; Thrall and Burdon, 2003), The wild type could also have higher growth rate to compensate its higher mortality rate in the presence of disease. All the above assumptions can be easily modified from our current models to explore these questions in future work.

In summary, our study highlights the necessity of studying the selection of pathogens on hosts (i.e., the dynamics of systems with evolving hosts but constant pathogen) and sheds light on the ecology-evolution interactions (e.g., Best et al., 2011; Brown and Hastings, 2003; Débarre et al., 2012; Lambrinos, 2004; Lion and Gandon, 2015; Schreiber et al., 2018). Our findings also demonstrate the importance of considering short-term host-pathogen transient dynamic during the design of conservation strategies. We contribute to a growing body of literature on the necessity of studying transient dynamics and regime change (Caswell, 2019; Hastings, 2001, 2004; Rabinovich et al., 2008; Shriver et al., 2019). By exploring the influence of host metapopulation on system evolution, our findings specifically provide guidance for manipulating migration to achieve biological conservation for populations under disease threat (see Jiao et al., 2018; Rolls, 2011; Subba et al., 2018)): e.g., either building corridors to facilitate migration, or deploy blocks to decrease migration, depending on the conservation purposes

and system dynamics at certain mortality levels (see the relationship between patch connectivity and migration; Fig. 6, Fig. S9 and S10 in Appendix 4). We present clear evidence that metapopulation dynamics and movement ecology must also be incorporated into evolutionary epidemiology when managing populations under threat from novel pathogens.

Declaration of competing interest

The authors declare that they have no known competing financial interests or personal relationships that could have appeared to influence the work reported in this paper.

Acknowledgements

This work was partially supported by NSF EEID/DEB 1717498 and 2001213 and we are grateful to Dr. Brooke Maslo for early conversations shaping this research.

Appendix A. Supplementary data

Supplementary data to this article can be found online at https://doi.org/10.1016/j.gecco.2020.e01174.

References

Anderson, R.M., May, R.M., 1979. Population biology of infectious diseases: Part I. Nature 280, 361–367.

Armsworth, P.R., Roughgarden, J.E., 2005. The impact of directed versus random movement on population dynamics and biodiversity patterns. Am. Nat. 165 (4) 449–465

Baalen, M.V., 1998. Coevolution of recovery ability and virulence. Proc. Roy. Soc. Lond. Ser. B Biol. Sci. 265, 317-325.

Beck, K., 1984. Coevolution: mathematical analysis of host-parasite interactions. J. Math. Biol. 19, 63–77.

Best, A., Webb, S., White, A., Boots, M., 2011. Host resistance and coevolution in spatially structured populations. Proc. Biol. Sci. 278, 2216-2222.

Best, A., White, A., Boots, M., 2008. Maintenance of host variation in tolerance to pathogens and parasites. Proc. Natl. Acad. Sci. Unit. States Am. 105, 20786–20791.

Best, A., White, A., Boots, M., 2010. Resistance is futile but tolerance can explain why parasites do not always castrate their hosts. Evol. Int. J. Organ. Evol. 64, 348–357.

Bliven, K.A., Maurelli, A.T., 2012. Antivirulence genes: insights into pathogen evolution through gene loss. Infect. Immun. 80, 4061-4070.

Boots, M., Bowers, R.G., 1999. Three mechanisms of host resistance to microparasites—avoidance, recovery and tolerance—show different evolutionary dynamics. J. Theor. Biol. 201, 13–23.

Boots, M., Haraguchi, Y., 1999. The evolution of costly resistance in host-parasite systems. Am. Nat. 153, 359-370.

Bowers, R.G., Boots, M., Begon, M., 1994. Life-history trade-offs and the evolution of pathogen resistance: competition between host strains. Proc. Roy. Soc. Lond. Ser. B Biol. Sci. 257, 247–253.

Bremermann, H.J., Pickering, J., 1983. A game-theoretical model of parasite virulence. J. Theor. Biol. 100, 411-426.

Brown, D.H., Hastings, A., 2003. Resistance may be futile: dispersal scales and selection for disease resistance in competing plants. J. Theor. Biol. 222, 373–388.

Carlsson-Granér, U., Thrall, P.H., 2006. The impact of host longevity on disease transmission: host—pathogen dynamics and the evolution of resistance. Evol. Ecol. Res. 8, 659–675.

Carlsson-Granér, U., Thrall, P.H., 2002. The spatial distribution of plant populations, disease dynamics and evolution of resistance. Oikos 97, 97-110.

Carlsson-Granér, U., Thrall, P.H., 2015. Host resistance and pathogen infectivity in host populations with varying connectivity. Evolution 69, 926–938.

Caswell, H., 2019. Sensitivity Analysis: Matrix Methods in Demography and Ecology. Springer.

Conner, M.M., Miller, M.W., 2004. Movement patterns and spatial epidemiology of a prion disease in mule deer population units. Ecol. Appl. 14, 1870–1881. Cramer, M.J., Willig, M.R., 2005. Habitat heterogeneity, species diversity and null models. Oikos 108, 209–218.

Danielson, B.J., 1991. Communities in a landscape: the influence of habitat heterogeneity on the interactions between species. Am. Nat. 138, 1105–1120. Débarre, F., Lion, S., Van Baalen, M., Gandon, S., 2012. Evolution of host life-history traits in a spatially structured host-parasite system. Am. Nat. 179, 52–63. Didelot, X., Walker, A.S., Peto, T.E., Crook, D.W., Wilson, D.J., 2016. Within-host evolution of bacterial pathogens. Nat. Rev. Microbiol. 14, 150.

Didelot, X., Walker, A.S., Peto, T.E., Crook, D.W., Wilson, D.J., 2016. Within-host evolution of bacterial pathogens. Nat. Rev. Microbiol. 14, 150. Earn, D.J., Rohani, P., Grenfell, B.T., 1998. Persistence, chaos and synchrony in ecology and epidemiology. Proc. Roy. Soc. Lond. Ser. B Biol. Sci. 265, 7–10.

Echaubard, P., Leduc, J., Pauli, B., Chinchar, V.G., Robert, J., Lesbarreres, D., 2014. Environmental dependency of amphibian—ranavirus genotypic interactions: evolutionary perspectives on infectious diseases. Evol. Appl. 7, 723—733.

Gause, G., 1970. Criticism of invalidation of principle of competitive exclusion. Nature 227, 89-89.

Gilchrist, M.A., Sasaki, A., 2002. Modeling host-parasite coevolution: a nested approach based on mechanistic models. J. Theor. Biol. 218, 289–308. Gillespie, J.H., 1975. Natural selection for resistance to epidemics. Ecology 56, 493–495.

Gonzalez, A., Ronce, O., Ferriere, R., Hochberg, M.E., 2013. Evolutionary Rescue: an Emerging Focus at the Intersection between Ecology and Evolution. The Royal Society.

Gordo, I., Gomes, M.G.M., Reis, D.G., Campos, P.R., 2009. Genetic diversity in the SIR model of pathogen evolution. PloS One 4.

Greenbaum, G., Fefferman, N.H., 2017. Application of network methods for understanding evolutionary dynamics in discrete habitats. Mol. Ecol. 26 (11), 2850–2863.

Hanski, I., 1999. Metapopulation Ecology. Oxford University Press.

Hastings, A., 2001. Transient dynamics and persistence of ecological systems. Ecol. Lett. 4, 215–220.

Hastings, A., 2004. Transients: the key to long-term ecological understanding? Trends Ecol. Evol. 19, 39–45.

Hess, G., 1996. Disease in metapopulation models: implications for conservation. Ecology 77, 1617–1632.

Holt, R.D., 1977. Predation, apparent competition, and the structure of prey communities. Theor. Popul. Biol. 12, 197–229.

Hossack, B.R., Russell, R.E., McCaffery, R., 2020. Contrasting demographic responses of toad populations to regionally synchronous pathogen (Batracho-chytrium dendrobatidis) dynamics. Biol. Conserv. 241, 108373.

Jiao, J., Pilyugin, S.S., Osenberg, C.W., 2016. Random movement of predators can eliminate trophic cascades in marine protected areas. Ecosphere 7, e01421. Jiao, J., Pilyugin, S.S., Riotte-Lambert, L., Osenberg, C.W., 2018. Habitat-dependent movement rate can determine the efficacy of marine protected areas. Ecology 99, 2485–2495.

Kimura, M., Weiss, G.H., 1964. The stepping stone model of population structure and the decrease of genetic correlation with distance. Genetics 49, 561. Laine, A.L., 2005. Spatial scale of local adaptation in a plant-pathogen metapopulation. J. Evol. Biol. 18, 930–938.

Lambrinos, J.G., 2004. How interactions between ecology and evolution influence contemporary invasion dynamics. Ecology 85, 2061–2070.

Levin, S., Pimentel, D., 1981. Selection of intermediate rates of increase in parasite-host systems. Am. Nat. 117, 308-315.

Levin, S.A., 1970. Community equilibria and stability, and an extension of the competitive exclusion principle. Am. Nat. 104, 413-423.

Lewis, I.W., 1981, On the coevolution of pathogen and host: I. General theory of discrete time coevolution, I. Theor. Biol. 93, 927–951.

Lion, S., Gandon, S., 2015. Evolution of spatially structured host–parasite interactions. J. Evol. Biol. 28, 10–28.

Maslo, B., Fefferman, N.H., 2015. A case study of bats and white-nose syndrome demonstrating how to model population viability with evolutionary effects. Conserv. Biol. 29, 1176-1185.

May, R.M., Anderson, R.M., 1983. Epidemiology and genetics in the coevolution of parasites and hosts, Proc. R. Soc. Lond. Ser. B Biol. Sci. 219, 281-313.

Medzhitov, R., Schneider, D.S., Soares, M.P., 2012, Disease tolerance as a defense strategy, Science 335, 936-941.

Miller, M., White, A., Boots, M., 2005. The evolution of host resistance: tolerance and control as distinct strategies. J. Theor. Biol. 236, 198-207.

Miller, M.R., White, A., Boots, M., 2006. The evolution of parasites in response to tolerance in their hosts: the good, the bad, and apparent commensalism. Evolution 60, 945-956.

Mittelbach, G.G., McGill, B.J., 2019. Community Ecology. Oxford University Press.

Mordecai, E.A., Jaramillo, A.G., Ashford, J.E., Hechinger, R.F., Lafferty, K.D., 2016. The role of competition—colonization tradeoffs and spatial heterogeneity in promoting trematode coexistence. Ecology 97, 1484-1496.

Nesse, R.M., Williams, G.C., 2012. Why We Get Sick: the New Science of Darwinian Medicine. Vintage.

North, A.R., Godfray, H.C.J., 2017. The dynamics of disease in a metapopulation: the role of dispersal range. J. Theor. Biol. 418, 57-65.

Payne, C., 1988, Pathogens for the control of insects: where next? Philos. Trans. R. Soc. Lond. B Biol. Sci. 318, 225–248.

Råberg, L., Graham, A.L., Read, A.F., 2009. Decomposing health: tolerance and resistance to parasites in animals. Phil. Trans. Biol. Sci. 364, 37–49.

Rabinovich, M., Huerta, R., Laurent, G., 2008. Transient dynamics for neural processing. Science 321, 48-50.

Restif, O., Koella, J.C., 2004. Concurrent evolution of resistance and tolerance to pathogens. Am. Nat. 164, E90-E102.

Rolls, R.J., 2011. The role of life-history and location of barriers to migration in the spatial distribution and conservation of fish assemblages in a coastal river system. Biol. Conserv. 144, 339–349. Roy, B., Kirchner, J., 2000. Evolutionary dynamics of pathogen resistance and tolerance. Evolution 54, 51–63.

Sanchez, J.N., Hudgens, B.R., 2019. Impacts of heterogeneous host densities and contact rates on pathogen transmission in the Channel Island fox (Urocyon littoralis). Biol. Conserv. 236, 593-603.

Schreiber, S.J., Patel, S., terHorst, C., 2018. Evolution as a coexistence mechanism; does genetic architecture matter? Am. Nat. 191, 407–420.

Seitz, R.D., Lipcius, R.N., Hines, A.H., 2017. Consumer versus resource control and the importance of habitat heterogeneity for estuarine bivalves. Oikos 126, 121 - 135

Shiga, T., 1988. Stepping stone models in population genetics and population dynamics. In: Stochastic Processes in Physics and Engineering. Springer, pp. 345-355.

Shriver, R.K., Andrews, C.M., Arkle, R.S., Barnard, D.M., Duniway, M.C., Germino, M.J., Pilliod, D.S., Pyke, D.A., Welty, J.L., Bradford, J.B., 2019. Transient population dynamics impede restoration and may promote ecosystem transformation after disturbance. Ecol. Lett. 22, 1357-1366.

Subba, B., Sen, S., Ravikanth, G., Nobis, M.P., 2018. Direct modelling of limited migration improves projected distributions of Himalayan amphibians under climate change. Biol. Conserv. 227, 352-360.

Tack, A.L., Horns, F., Laine, A.L., 2014. The impact of spatial scale and habitat configuration on patterns of trait variation and local adaptation in a wild plant parasite. Evolution 68, 176–189.

Thompson, J.N., 1999. Specific hypotheses on the geographic mosaic of coevolution. Am. Nat. 153, S1-S14.

Thrall, P.H., Burdon, J.J., 1999. The spatial scale of pathogen dispersal: consequences for disease dynamics and persistence. Evol. Ecol. Res. 1, 681-701.

Thrall, P.H., Burdon, J.J., 2003. Evolution of virulence in a plant host-pathogen metapopulation. Science 299, 1735–1737.

Tilman, D., 1990. Constraints and tradeoffs: toward a predictive theory of competition and succession. Oikos 3-15.

Wild, G., Gardner, A., West, S.A., 2009. Adaptation and the evolution of parasite virulence in a connected world. Nature 459, 983-986.